

## **A QUADRATIC PETROV-GALERKIN FORMULATION FOR ADVECTION-DIFFUSION-REACTION PROBLEMS IN TURBULENCE MODELLING**

ALESSANDRO CORSINI, FRANCO RISPOLI AND ANDREA SANTORIELLO  
Department of Mechanics and Aeronautics, University of Rome “La Sapienza”  
I00184 Rome, Italy  
`corsini@dma.ing.uniroma1.it`

[Received: November 12, 2003]

**Abstract.** A new stabilized FEM formulation for advective-diffusive-reactive problems is presented. The new method, called Spotted Petrov-Galerkin (SPG), combines two perturbations of quadratic Galerkin weight function: the first one is a generalized SUPG operator, the second one a nodal spot-like controlling operator designed for reactive instabilities. The formulation covers all the combinations of advective and reactive effects, associated with the dimensionless element Peclet and reaction numbers. After an introduction to the method, we assess the reliability of SPG in the control of reactivity related oscillations both in model problems and in turbomachinery turbulence modelling. In the numerical experiments the SPG performance has been compared to classical stabilization schemes, e.g. SUPG.

*Mathematical Subject Classification:* 76F99, 76M10

*Keywords:* reaction effects, stabilized finite element method, turbulence modelling

### **1. Introduction**

In this work we focus on the numerical solution of advective-reactive-diffusive problems using the Finite Element Method (FEM) on quadratic space of approximation. Here, diffusion, advection and reaction refer to the terms in the partial differential equations (PDEs) involving second, first and zero order derivatives of the unknowns. This family of equations that governs several phenomena of industrial interest is discussed here because of its importance in the modelling of turbomachinery fluid dynamics.

Several sources of oscillations affect the solution of PDEs in fluid dynamics if standard schemes are used (e.g. central finite differences or Galerkin finite elements). In the finite element framework a number of stabilized formulations have been proposed during the last two decades as remedial strategies. Most of them were based on a Petrov-Galerkin (PG) approach, where the stabilization is achieved preserving the Euler-Lagrange condition's consistency by adding a perturbation to the Galerkin weights (such as SUPG [1-4], or PSPG [3], or Discontinuity Capturing [5] schemes).

An additional origin of instabilities stems from the reaction or zero order derivative terms. Local oscillations arise near boundaries or solution discontinuities and it is not possible to obtain a global stability estimate in the  $H^1$  norm, though it could be evaluated in  $L^2$  [6]. Moving towards the turbomachinery CFD, these terms are usually related to the rotation of turbomachinery frame of reference (e.g. in the modelling of Coriolis forces), but it is worth noting that they appear also in an absorption-like fashion in the turbulence modelling closure equations (e.g. two equations eddy viscosity models (EVM)).

To the best of the authors' knowledge, in the open literature only equal order PG formulations have been developed to control advective-diffusive-reactive flow problems, dealing with scalar equations (e.g. (SU+C)PG in [7]) or linear reactive operators [8]. Few studies are concerned with reactive problems pertinent to real turbomachinery fluid dynamics [6].

From this viewpoint, the present work addresses the definition of a new Petrov-Galerkin stabilization scheme for the reactive flow limit, formulated on a quadratic finite element space of approximation. The use of a higher order stabilized formulation, though its complexity is due to the non-negligibility of second order derivatives, guarantees the best compromise between solution stability and accuracy [9]. In particular, the authors propose a stabilized formulation that performs well both in the advection and in the reaction dominated case. The new method is called *Spotted Petrov-Galerkin* (SPG) and possesses some distinctive features. For advection-diffusion problems it behaves like a SUPG method, whereas in the reactive-diffusive limit the space invariant problem is controlled by a perturbation able to give rise to spot-like weight functions, symmetric and concentrated around each nodal position. In intermediate situations, the scheme combines the perturbation integrals using tuning or *upwind* coefficients that depend on element Peclet and reaction numbers.

The remainder of the paper is organized as follows. In Section 2 the SPG formulation is presented for linear scalar advective-diffusive-reactive equations. The extension of the formulation to multi-dimensional case is discussed, and the family of weights for Q2 element is shown. In Section 3 the reactivity features of general PDE that models the budget of turbulent determining-scale variables are commented on. Finally in Section 4 the performance of SPG is assessed in three test cases against solutions provided by SUPG, Streamline Upwind or Galerkin.

## 2. Finite element scalar advective-diffusive-reactive problem

**2.1. Introductory remarks.** Let us take the general linear scalar advective-reactive-diffusive problem statement on the closed domain  $\underline{\Omega}$  for the unknown  $\phi$ :

$$\begin{aligned} u_j \phi_{,j} - k \phi_{,jj} + c \phi &= f, & (j = 1, nsd) \\ \phi(\Gamma_g) &= \phi_g, \\ \phi_{,n}(\Gamma_h) &= \theta_n, \end{aligned} \tag{2.1}$$

where  $nsd$  is the number of space dimensions,  $k > 0$  is constant diffusivity,  $u_j$  are the velocity components,  $c \geq 0$  is the reaction coefficient, and  $f$  is the source term. The

boundary conditions are specified along  $\Gamma = \underline{\Gamma}_h \cup \underline{\Gamma}_g$  ( $\underline{\Gamma}_h$  and  $\underline{\Gamma}_g$  are closed, disjoint subsets of  $\Gamma$ ), including Dirichlet ( $\phi_g$ ) and Neumann conditions ( $\theta_n$ ).

A finite element partition of the original closed domain  $\underline{\Omega}$  into elements  $\Omega_e, e = 1, nel$  ( $nel$  number of elements) reads as

$$\cup_e \Omega_e = \Omega \quad \text{and} \quad \cap_e \Omega_e = \emptyset \tag{2.2}$$

with the definition of interior boundary as  $\Gamma_{int} = \cup_e \Gamma_e - \Gamma$ .

Let us define the finite dimensional spaces of trial and weight functions as:

$$S^h = \phi^h | \phi^h \in H^{1h}(\Omega), \phi^h = \phi_g \text{ on } \Gamma_g, \quad \phi_g \in H^{(1/2)h}(\Gamma_g) \tag{2.3}$$

$$W^h = \{ w^h | w^h \in H_0^{1h}, w^h = 0 \text{ on } \Gamma_g \} \tag{2.4}$$

where  $H^{1h}(\Omega)$  and  $H_0^{1h}(\Omega)$  are the Sobolev spaces for the continuous pair of finite element functions,  $H^{(1/2)h}(\Gamma_g)$  is their restriction to the domain boundary, and the superscript  $h$  denotes the characteristic length scale of the domain discretization.

The Galerkin weak formulation of problem (2.1) reads as follows:

$$\begin{aligned} \sum_{e=1}^{nel} \int_{\Omega_e} w^h u_j \phi_{,j}^h d\Omega + \sum_{e=1}^{nel} \int_{\Omega_e} w_{,j}^h k \phi_{,j}^h d\Omega + \\ \sum_{e=1}^{nel} \int_{\Omega_e} w^h c \phi^h d\Omega = \sum_{e=1}^{nel} \int_{\Omega_e} w^h f d\Omega + \int_{\Gamma_h} w^h k \frac{\partial \phi^h}{\partial n} d\Gamma . \end{aligned} \tag{2.5}$$

**2.2. Galerkin formulation in one dimension.** Let us consider the ordinary differential equation obtained from (2.1) for  $nsd = 1$  and source term  $f = 0$ . The problem statement reads as:

$$u \frac{d\phi}{dx} - k \frac{d^2\phi}{dx^2} + c\phi = 0 , \tag{2.6}$$

The discretization of (2.6) by using the Galerkin method on a quadratic space of interpolation with uniform elements of length  $h$ , in case of constant coefficients leads to the following difference equations:

$$\phi_{i-1}[-4 - 2Pe + r/10] + \phi_i[8 + r4/5] + \phi_{i+1}[-4 + 2Pe + r/10] = 0 \tag{2.7}$$

if ( $i$ ) is chosen as element central node and

$$\begin{aligned} \phi_{i-2}[1 + Pe - r/10] + \phi_{i-1}[-8 - 4Pe + r/5] + \\ \phi_i[14 + r4/5] + \phi_{i+1}[-8 + 4Pe + r/5] + \phi_{i+2}[1 - Pe - r/10] = 0 \end{aligned} \tag{2.8}$$

if ( $i - 2, i, i + 2$ ) are chosen as element extreme nodes.

In the above equations, the magnitudes of advection or reaction versus diffusion are, respectively, given by element Peclet number  $Pe = ||u|| h/2k$ , and element reaction number  $r = ch^2/k$ .

Let us now focus on the element central node ( $i$ ). Now the null advection limit equation (2.7) reads as:

$$\phi_{i-1}[-4 + r/10] + \phi_i[8 + r4/5] + \phi_{i+1}[-4 + r/10] = 0. \quad (2.9)$$

The solutions of the characteristic equation associated with (2.9), which are the so-called Galerkin nodal amplification factors [8], purely depend on the magnitude of reaction:

$$\rho = \frac{-(8 + \frac{4}{5}r) \pm \sqrt{(8 + \frac{4}{5}r)^2 - 4(-4 + \frac{r}{10})^2}}{2(-4 + \frac{r}{10})} \quad (2.10)$$

where it could be easily seen that the exact solution exponential behavior is preserved only with  $r < 40$ . This circumstance confirms the need for a stabilized scheme with built-in component to preclude oscillatory behavior in reaction dominated cases.

**2.3. SPG formulation.** The stabilized SPG formulation is obtained by imposing nodal exactness on the numerical solution of problem (2.6). Provided that different equations have been obtained for the extreme and central nodes [4], it is possible to find two optimal perturbations, on the basis of the discrete equations (2.7) and (2.8) separately.

The PG weight functions now result from the addition to the Galerkin ones  $w_i$  of two perturbations  $P_{1i}$  and  $P_{2i}$  as:

$$\tilde{w}_i = w_i + \alpha P_{1i} + \gamma P_{2i} \quad (2.11)$$

with  $\alpha$  and  $\gamma$  being the tuning coefficients for element central nodes, and

$$\tilde{w}_i = w_i + \beta P_{1i} + \eta P_{2i} \quad (2.12)$$

with  $\beta$  and  $\eta$  being the tuning coefficients for element extreme nodes.

The first perturbation is formally similar to a SUPG one and reads as:

$$P_{1i} = \frac{h}{2\|u\|} u_k w_{,k}. \quad (2.13)$$

On the other hand, the design of  $P_{2i}$  is based on the following constraints. First, in *null advection* case the invariance of the equation under coordinate inversion suggests preserving the weight symmetry [7]. Moreover, in the *pure reaction* limit ( $r \rightarrow \infty$ ), the optimal weight would be a Dirac's delta. On this basis, the expression of  $P_{2i}$  suggested by the authors is a polynomial of the sixth order, negative definite inside each element:

$$P_{2i} = -\frac{C_{SPG}}{h^6} [\xi^6 - \frac{h^2}{2}\xi^4 + \frac{h^4}{16}\xi^2], \quad (2.14)$$

where  $\xi$  represents the coordinate in the master or logic space, and the coefficient  $C_{SPG}$  sets the asymptotic values of reactive tuning functions  $\gamma$  and  $\eta$ , without affecting  $\alpha$  and  $\beta$ .

Figure 1 shows the perturbation  $P_{2i}$  and the resulting weight functions for nodes of two neighboring elements, for one-dimensional quadratic elements in case of null advection with varying  $\gamma$  and  $\eta$  coefficients. The weights are plotted for  $C_{SPG} = (2^{12}/3^2) \times 0.35$ . This value stems from the fulfillment of seven constraints for  $P_{2i}$

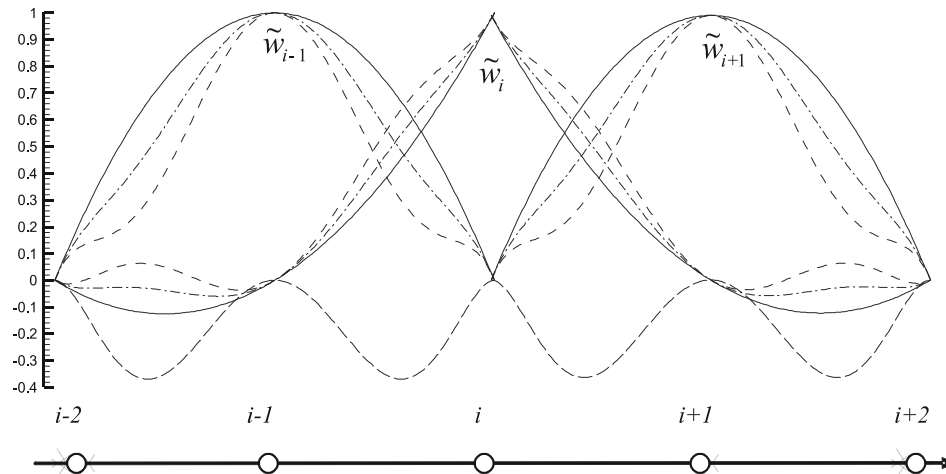


Figure 1. 1D null advection. Resulting nodal weights for neighboring elements (solid lines:  $\gamma = -2\eta = 0$ ; dashdot lines:  $\gamma = -2\eta = 0.5$ ; dashed lines:  $\gamma = -2\eta = 1$ ; longdash lines:  $P_{2i}$  function)

perturbation on quadratic elements, including null nodal values and derivatives, and  $P_{2i}$  magnitude at  $\xi = \pm h/4$ .

The expression for the tuning functions  $\alpha$  and  $\gamma$ , and  $\beta$  and  $\eta$  are consequent to the super-convergence condition. Figures 2.a and 2.b show the behaviors of  $\alpha$  and  $\gamma$  for different combinations of  $Pe$  and  $r$ . Furthermore, Figures 3a and 3b show those of  $\beta$  and  $\eta$  tuning functions.

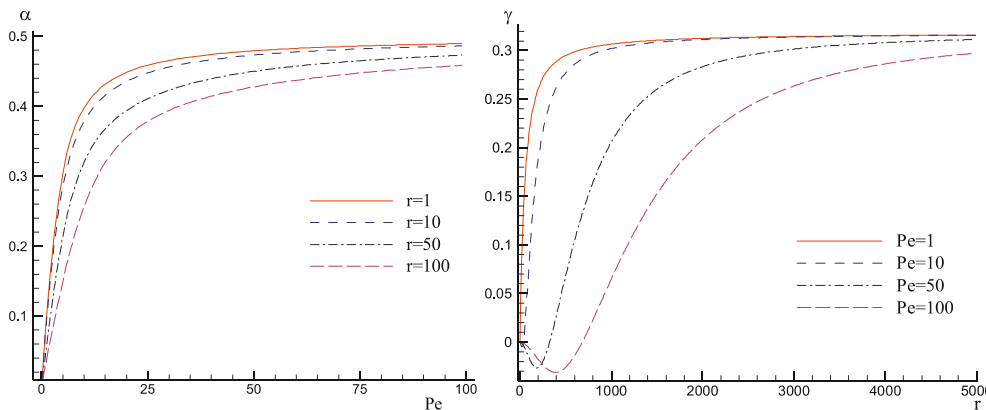


Figure 2. Tuning functions: a)  $\alpha$  and b)  $\gamma$

**2.4. Extension of SPG formulation to multi-dimensional case.** The 2D extension of the  $P_{2i}$  function has been designed to preserve its 1D requirement, that is the isotropic concentration of the perturbed weight around the nodal positions. To this end, we designed a Cartesian product between the 1D counterparts of the second

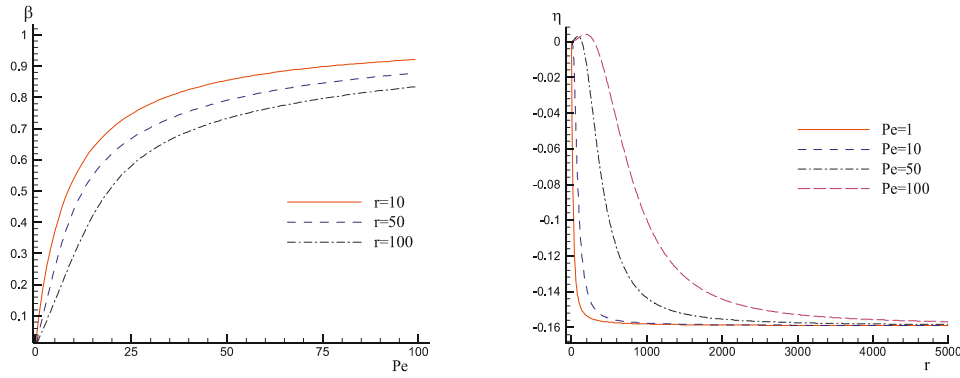


Figure 3. Tuning functions: a)  $\beta$  and b)  $\eta$

perturbation function, where the  $P_{2i}$  spots are moved in the element portion closer to the corresponding nodes.

This concept is depicted in Figure 4, which shows the resulting geometries for the two-dimensional second perturbation functions on logic space.

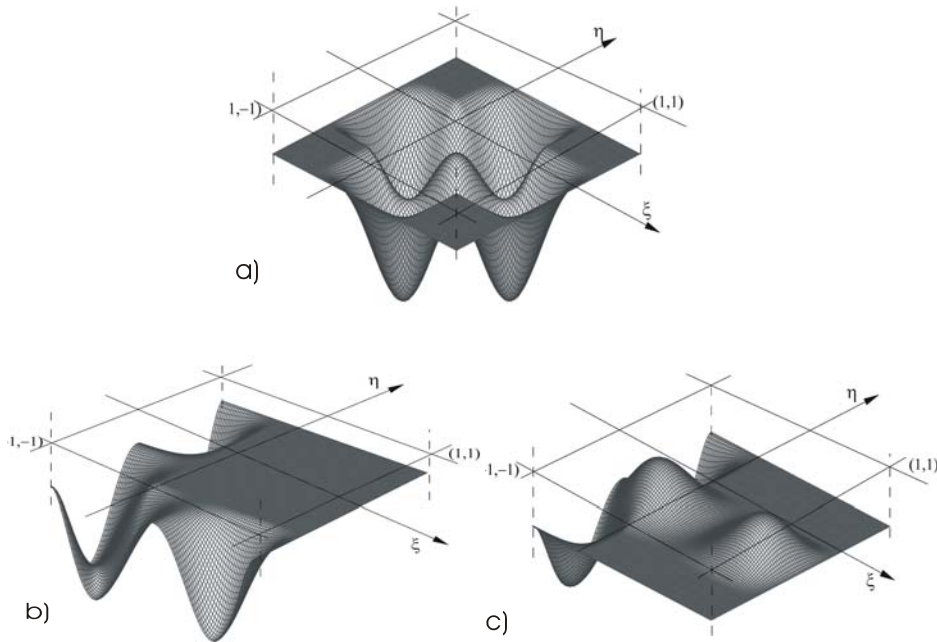


Figure 4. 2D  $P_{2i}$  functions in the logic space: a) central-central node  $(0,0)$ , b) corner node  $(-1,-1)$ , c) mid-side node  $(-1,0)$

### 3. Problem statement for EVM

Let us now examine the determining-scale equations in a first moment turbulence closure. The general steady-state advective-diffusive-reactive equation used to model the budget of a turbulent variable  $\phi$  (i.e.  $\phi$  could represent the turbulent viscosity  $\nu_t$ , the turbulent kinetic energy  $k$ , or the dissipation  $\varepsilon$ ) reads as:

$$F_{\phi a} + F_{\phi d} = P_\phi + \varepsilon_\phi + S_\phi \tag{3.1}$$

here:  $F_{\phi a}$  are the convective fluxes,  $F_{\phi d}$  are the diffusive fluxes,  $P_\phi$  is the production,  $\varepsilon_\phi$  is the dissipation (or destruction) term, and  $S_\phi$  is the term containing the near wall extra sources. When the standard  $k - \varepsilon$  model proposed by Launder and Sharma (1974) [10] is used, the budget structure (3.1) gives rise to the terms sketched in Table 1.

Table 1.  $k - \varepsilon$  turbulence model equations; budget

	$k$	$\varepsilon$
$F_{\phi a}$	$\rho u_j k_{,j}$	$\rho u_j \varepsilon_{,j}$
$F_{\phi d}$	$-\left[\left(v + \frac{\nu_t}{\sigma_k}\right)k_{,j}\right]_{,j}$	$-\left[\left(v + \frac{\nu_t}{\sigma_\varepsilon}\right)\varepsilon_{,j}\right]_{,j}$
$P_\phi$	$\nu_t[u_{i,j} + u_{j,i}]u_{i,j}$	$c_1 f_1 \frac{\varepsilon}{k} \nu_t [u_{i,j} + u_{j,i}]u_{i,j}$
$\varepsilon_\phi$	$-\frac{\varepsilon}{k}k$	$-c_2 f_2 \frac{\varepsilon}{k}k$
$S_\phi$	0	$E = 2 \nu \nu_t \left(\frac{\partial^2 u_i}{\partial x_j \partial x_k}\right)^2$

In Table 1:  $\nu_t = c_\mu f_\mu k^2/\varepsilon$  is the scalar eddy viscosity;  $f_1, f_2, f_\mu$  are damping functions;  $c_1, c_2, c_\mu, \sigma_k, \sigma_\varepsilon$  are empirical constants. The extra term  $E$  is the buffer-layer source to correct the near wall dissipation behaviour.

It is worth mentioning that in the numerical approach developed, the dissipation integrals  $\varepsilon_\phi$  explicitly contain the reaction terms and, for the EVM under study, they are made proportional to the inverse of turbulence time scale  $\tau = k/\varepsilon$ . These integrals are included as left-hand side (LHSV) contributions to the coefficient matrix. By that way a strong coupling is built between the  $k - \varepsilon$  determining-scale equations in order to improve the solver convergence.

### 4. Numerical examples

**4.1. The examples presented.** In this section we assess the numerical performance of the proposed SPG formulation for model problems and for configurations pertinent to turbomachinery fluid dynamics. In these validation studies the improvement of the SPG are discussed with respect to the classical stabilization schemes, such as the SUPG or Streamline Upwind. It is remarkable that, since all the stabilization schemes usually share the optimum property in 1D, all the investigated test cases violate one of the super-convergence conditions (i.e. non-uniform mesh, multidimensional domain, non-linear equations and problems with source terms).

**4.2. Scalar advective-diffusive-reactive equation on a square domain.** The first test cases (labeled TC1 and TC2) concern the numerical solution of the linear scalar advective-diffusive-reactive model problem (2.1), in a unit square domain. The mesh is uniform with  $10 \times 10$  quadratic elements, thus consisting of 441 nodes. For both TC1 and TC2 the known velocity field  $u$  is assumed to have a parabolic profile (e.g.  $u(x, y) = 2y - y^2$ ,  $v(x, y) = 0$ ), with maximum value equal to 1. The coefficients are:  $k = 10^{-5}$ ,  $c = 5 \times 10^2$ . The maxima for dimensionless element numbers are:  $Pe = o(10^3)$  and  $r = o(10^5)$ . As concerns the source term, TC1 has null  $f$  value, whereas in TC2 a non-uniform  $f$  has been adopted with a peak value equal to  $50 \phi_{BC}$ . For both the test cases the SPG solutions are compared to quadratic Galerkin (G Q2), and SUPG Q2 ones. Concerning TC1, the complete problem statement and the solution fields for Galerkin and SPG are shown in Figure 5.

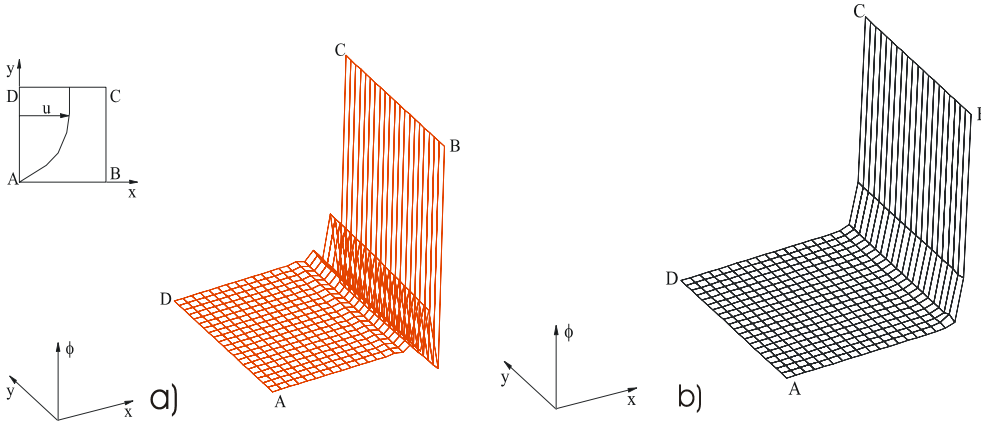


Figure 5. Scalar advective-diffusive-reactive problem statement TC1 ( $f = 0$ ) and solution fields: a) G Q2 and b) SPG

As it clearly appears, the proposed SPG formulation is able of controlling completely the instability origins in the near- and far-wall regions. Figure 6 shows the  $\phi$  streamwise profiles predicted by G Q2, SUPG Q2 and SPG schemes at  $y = 0.05$  where reaction dominates. The PG-like solutions are both able to predict smooth  $\phi$  profiles, thus improving the G Q2 oscillatory behaviour. Nonetheless, the SUPG Q2 returns an over-diffused layer close to the Dirichlet bound. This confirms its inability to control the reactive effects, with respect to SPG solution that predicts a sharp but continuous solution layer.

As far as the TC2 case is concerned, in Figure 7 the problem statement and the SUPG Q2 and SPG solutions are shown. It is worth noting that the source integral has been approximated linearly, according to Q2 element optimal conditions [4].



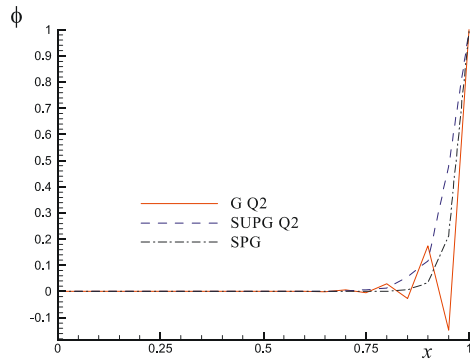


Figure 6. TC1 comparison of streamwise  $\phi$  profiles at  $y = 0.05$

Moreover, Figure 8 shows the  $\phi$  streamwise profiles predicted by G Q2, SUPG Q2 and SPG schemes at  $y = 0.05$ , where the reactive effect is combined with a positive gradient of the source.

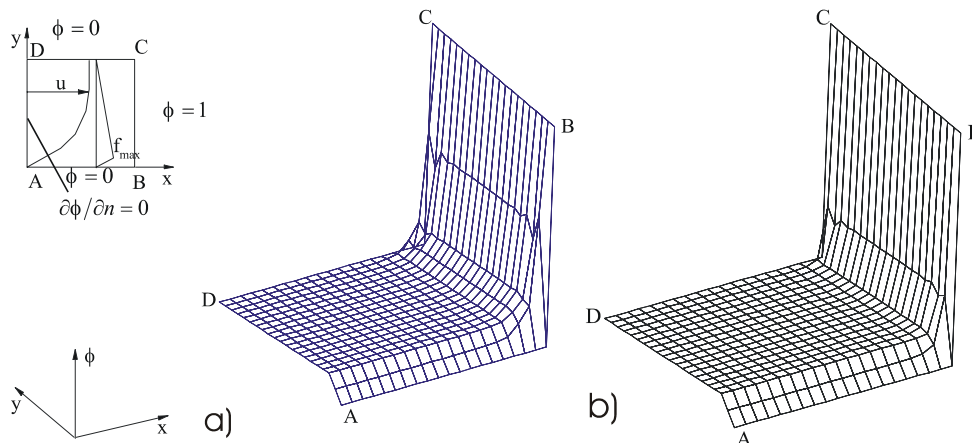


Figure 7. Scalar advective-diffusive-reactive problem statement TC2 ( $f_{max}(y=0.1) = 50$ ) and solution fields: a) SUPG Q2 and b) SPG

The comparison between stabilized PG schemes confirms that the SPG is able to totally recover a non-oscillatory solution, also where the sharp streamwise solution layer develops under the effect of a non-uniform source.

**4.3. Semi-circular leading edge.** The last test case concerns the prediction of the turbulent boundary layer development on a flat plate, with a semi-circular leading edge. The leading edge configuration is that proposed by ERCOFTAC Special Interest Group on Transition in 1991 (labelled T3L). The experimental data have been provided by Palikaras et al. [11], for the zero pressure gradient configuration.

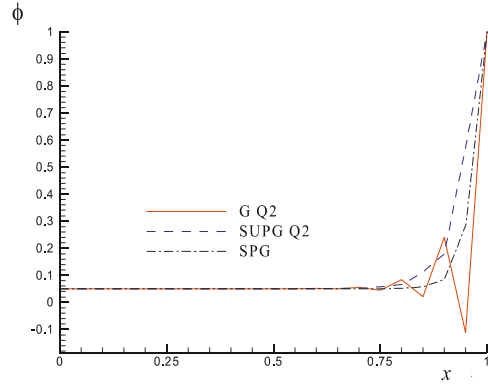


Figure 8. TC2 comparison of streamwise  $\phi$  profiles at  $y = 0.05$

The Reynolds number, based on inlet velocity and leading edge radius ( $e_r = 5\text{ mm}$ ) is equal to 1660. The free stream turbulence intensity (TI) at the inlet is set to 7%, and the chosen dissipation length  $l_\varepsilon$  is  $18\text{ mm}$ .

The flow is assumed two-dimensional with constant temperature and incompressible. A 12681 node block-structured (H-O) grid has been used. In the vicinity of the wall (O-connected region) the nearest node to the solid wall has a dimensionless distance  $\delta^+ = 1.0$ . At the inlet section of the computation domain, the experimental free-stream uniform profile is used for the mean velocity ( $u = 5\text{ m/s}$ ). Uniform distributions are also imposed on the turbulent variables, computed on the basis of TI and  $l_\varepsilon$ . No-slip conditions are then applied on the solid surface, and homogeneous Neumann conditions are imposed at the outlet section.

The SUPG and SPG formulations have been used on Q2Q1 elements, with PSPG-like relaxation of incompressibility constraint. The turbulence closure is the standard  $k - \varepsilon$  model [10], in its near wall extension. A GMRes(50) solver has been used with convergence thresholds for error  $R_{res}$  and solution  $R_{sol}$  residuals set to  $10^{-6}$ . The convergence histories are first compared in Figure 9, clearly showing the faster convergence of SPG compared to the SUPG scheme. Figures 10 and 11 show the streamwise turbulence intensity and velocity profiles computed in two locations close to the leading edge stagnation point at  $x/e_r = 2.4$  and  $x/e_r = 3.2$ , respectively. The predicted velocity and turbulence intensity profiles agree with published numerical studies using isotropic EVMs (e.g. [10]). To this end, the stabilized formulations are able to give a good prediction of the free-stream values. Notwithstanding, the near wall region is affected by an over-prediction of TI level and layer thickness related to the stagnation point anomaly [12]. With respect to the comparative performance between PG schemes, the solutions do not show appreciable differences, as shown in Figures 10 and 11.

This evidence confirms that in a flow region dominated by the effect of advection, such as the flat plate region downwind the leading edge, where the maximum reaction

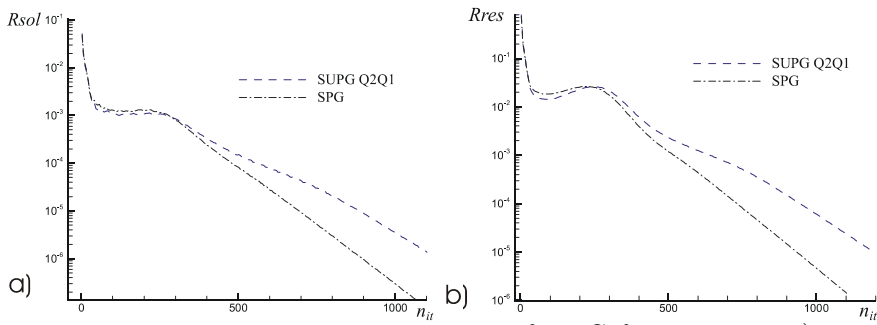


Figure 9. T3L convergence histories for PG formulations: a)  $R_{sol}$  and b)  $R_{res}$

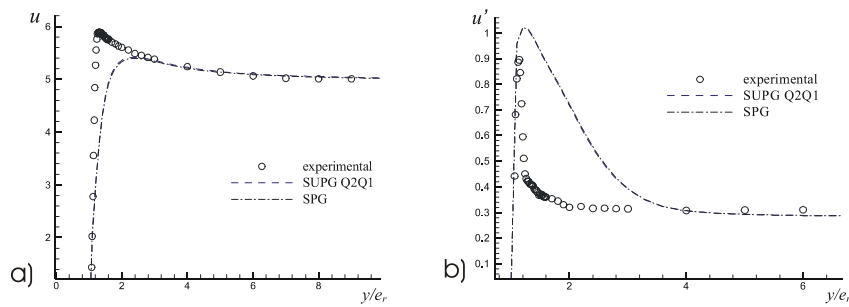


Figure 10. Comparison of streamwise: velocity  $u(m/s)$  a) and turbulence intensity  $u'(m/s)$  b) at  $x/e_r = 2.4$

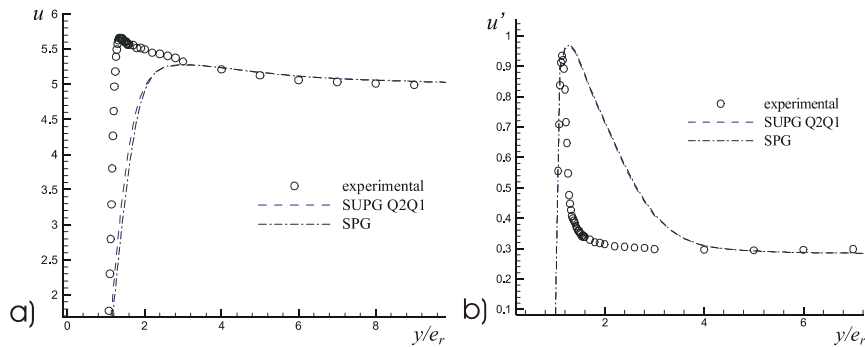


Figure 11. Comparison of streamwise: velocity  $u(m/s)$  a) and turbulence intensity  $u'(m/s)$  b) at  $x/e_r = 3.2$

number is of  $o(10^2)$ , the SPG correctly annihilates its sensitivity to the equation reactivity recovering a SUPG-like behaviour. Moving upwind in the stagnating flow region, some distinguishing feature of the proposed SPG could be found. To this end

in Figures 12 and 13 are compared, respectively, the computed  $TI$  and turbulence time scale profiles along the stagnation streamline.

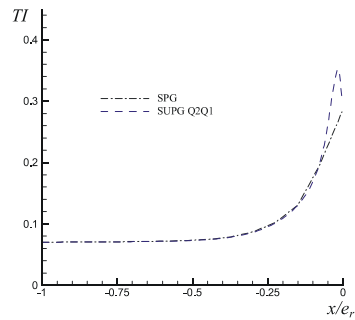


Figure 12. Comparison of  $TI$  profiles along the stagnation streamline

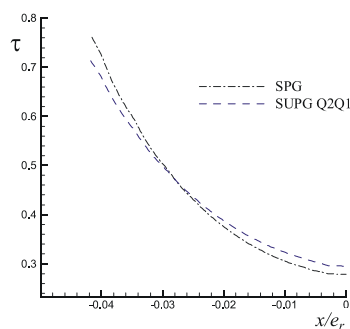


Figure 13. Comparison of  $\tau$  profiles along the stagnation streamline

The comparison of turbulence intensity profiles, in Figure 12, demonstrates that the SPG is able to reduce the  $TI$  peak ( $TI_{SPG} = 28\%$  instead  $TI_{SUPG} = 36\%$ ). This suggests that approaching a null-advection region, the SPG partially corrects one of the well recognized drawbacks of linear two-equation EVMs, the so-called stagnation point anomaly. Figure 13 shows that this remarkable feature of SPG formulation is related to the capacity of controlling the over-prediction of turbulence time scale in the pure reactive-diffusive flow limit. In this condition, the SPG perturbation activates a dependence of weights from the predicted turbulence scale intensity able to affect the corresponding residual projection basis.

## 5. Conclusions

The paper investigated the prediction capabilities of a FEM stabilized formulation developed for the purpose of solving advective-diffusive-reactive problems. This scheme, called SPG, addresses the use of a perturbation to the weight function composed by

two contributions. The first is a SUPG-like operator and is used to overcome instabilities due to advective or skew-symmetric terms, whereas the second operator is a symmetric one aiming at precluding oscillations due to reactive terms. The FEM formulation has been obtained by means of one-dimensional nodal exactitude, but has been tested in several more complex examples that violate the super convergence conditions. In this respect, the SPG method demonstrates its suitability for solving the typical equations of turbulence EVMs used in turbomachinery CFD.

**Acknowledgement.** The authors acknowledge MIUR under the projects COFIN 2001, and MIUR-Ateneo 2001.

## REFERENCES

1. HUGHES, T.J.R. AND BROOKS, A.N.: Streamline Upwind/Petrov-Galerkin formulations for convection dominated flows with particular emphasis on the incompressible Navier-Stokes equations. *Comp. Meth. Appl. Mech. Eng.*, **32**, (1982), 199–259.
2. HUGHES, T.J.R. AND BROOKS, A.N.: A theoretical framework for Petrov-Galerkin methods with discontinuous weighting functions: application to the streamline-upwind procedure. *Finite Elements in Fluids*, **4**, (1982), 47–65.
3. TEZDUYAR, T.E., MITTAL, S., RAY, S.E. AND SHIH, R.: Incompressible flow computations with stabilized bilinear and linear equal-order-interpolation velocity-pressure elements. *Comp. Meth. Appl. Mech. Eng.*, **95**, (1992), 221–242.
4. CODINA, R., OÑATE, E. AND CERVERA, M.: The intrinsic time for the streamline upwind/Petrov-Galerkin formulation using quadratic elements. *Comp. Meth. Appl. Mech. Eng.*, **94**, (1992), 239–262.
5. HUGHES, T.J.R., MALLETT, M. AND MIZUKAMI, A.: A new finite element formulation for computational fluid dynamics: II. Beyond SUPG. *Comp. Meth. Appl. Mech. Eng.*, **54**, (1986), 341–355.
6. CODINA, R.: A stabilized finite element method for generalized stationary incompressible flows. *Comp. Meth. Appl. Mech. Eng.*, **190**, (2001), 2681–2706.
7. IDELSOHN, S., NIGRO, N., STORTI, M. AND BUSCAGLIA G.: A Petrov-Galerkin formulation for advection-reaction-diffusion problems. *Comp. Meth. Appl. Mech. Eng.*, **136**, (1996), 27–46.
8. HARARI, I., AND HUGHES, T.J.R.: Stabilized finite element methods for steady advection-diffusion with production. *Comp. Meth. Appl. Mech. Eng.*, **115**, (1994), 165–191.
9. BORELLO, D., CORSINI, A. AND RISPOLI, F.: A finite element overlapping scheme for turbomachinery flows on parallel platforms. *Computers & Fluids*, **32**(7), (2003), 1017–1047.
10. LAUNDER, B.E., AND SHARMA, B.I.: Application of the energy dissipation model of turbulence to the calculation of flow near a spinning disc. *Letter in Heat and Mass Transfer*, **1**, (1974), 131–138.
11. PALIKARAS, A., YAKINTHOS, K. AND GOULAS, A.: Transition on a flat plate with a semi-circular leading edge under uniform and positive shear free-stream flow. *Int. J. Heat Fluid Flow*, **23**, (2002), 455–470.
12. DURBIN, P.A.: On the  $k-\varepsilon$  stagnation point anomaly. *Int. J. of Heat and Fluid Flow*, **17**, (1996), 89–90.